Forest Pathology

WILEY

Forest Pathology

ORIGINAL ARTICLE

Beech Leaf Disease Impairs Growth and Carbohydrate Storage in *Fagus grandifolia*

Cameron D. McIntire[1] | Andrew L. Loyd[2,3] | Chad M. Rigsby[2,4] | Patrick Lemis[5] | Elena Karlsen-Ayala[6] | Caitlin Littlejohn[2] | Aaron Bergdahl[7] | Jeff R. Garnas[5]

[1]Forest Health Protection, State, Private, & Tribal Forestry, USDA Forest Service, Durham, New Hampshire, USA | [2]Bartlett, Tree Research Laboratories, Charlotte, North Carolina, USA | [3]Botanical Research Institute of Texas, Fort Worth, Texas, USA | [4]The Morton Arboretum, Lisle, Illinois, USA | [5]Department of Natural Resources, University of New Hampshire, Durham, New Hampshire, USA | [6]Northern Research Station, USDA Forest Service, Hamden, Connecticut, USA | [7]Maine Forest Service, Department of Agriculture, Conservation, and Forestry, Augusta, Maine, USA

Correspondence: Cameron D. McIntire (cameron.mcintire@usda.gov)

Received: 25 November 2025 | **Revised:** 5 February 2026 | **Accepted:** 9 February 2026

Keywords: BLD | dendrochronology | ectomycorrhizae | *Litylenchus crenatae mccannii* | nematode | non-structural carbohydrates

ABSTRACT

Beech leaf disease (BLD) is a foliar disease of American beech (*Fagus grandifolia*) that manifests as gall symptoms in leaves caused by infestations from *Litylenchus crenatae* ssp. *mccannii,* a plant-parasitic nematode. As the disease progresses, infestations lead to bud abortion, crown deterioration and branch dieback. While BLD is known to impair leaf function, the impacts of the disease on tree carbon allocation and growth are unresolved. Here, we sampled three forest stands across a gradient of disease severity to assess how BLD influences the storage of non-structural carbohydrates (NSC) across different tissue pools (root, bole and twigs), used tree rings to estimate growth declines associated with the onset of BLD infestation and evaluated the fine root ectomycorrhizal communities. Our data show that BLD can negatively impact NSC storage across tissue pools in stands exhibiting both low- and high-severity infestation. Diminished starch content with respect to the asymptomatic stand was shown to precede any reduction in growth, measured via post-infestation basal area increment at the low-severity stand (1–2 years of infestation). Growth reductions at the high-severity stand (3+ years post infestation) were significant and coincided with low NSC content, though mortality was not observed among any mature trees. Root-associated fungal community composition differed significantly among sites, with a trend towards reduced diversity in more severely impacted trees. Our results suggest that BLD disrupts carbon allocation and storage in beech trees, potentially compromising their resilience to future stressors. The complex interplay between nematode infestation, fungal community shifts and altered carbohydrate dynamics highlights the multifaceted nature of BLD and its potential long-term consequences for beech forests.

1 | Introduction

American beech (*Fagus grandifolia* Ehrl) is a foundational tree species throughout eastern North America that represents 27.4% of forest understories and midstories throughout Maine, New Hampshire, New York and Vermont (Bose et al. 2017). Mature beech also produces a hard mast that is a critical source of nutrition for many native wildlife species in the eastern region (McNulty and Masters 2005; Storer et al. 2005). Beech leaf disease (BLD) in North America has been attributed to the foliar parasitic nematode *Litylenchus crenatae* ssp. *mccannii* (*Lcm*), which infests the buds and leaves of trees within the *Fagus* genus (Carta et al. 2020; Ewing et al. 2019). BLD is not endemic to North America; it was first detected in Ohio in 2012 and has since expanded rapidly across the eastern United States and southeastern Canada. Established infestations now occur from Michigan in the west to Maine in the northeast and as far south as North Carolina, with additional

spread north into Ontario, Canada. This expanding distribution has coincided with sapling mortality, progressive canopy thinning, and structural changes in long-infested stands (Reed et al. 2022; Shepherd et al. 2025). Susceptible host species include American beech, European beech (*F. sylvatica* L), Chinese beech (*F. engleriana* Seemen ex Diels) and Oriental beech (*F. orientalis* Lipsky). The closely related and earlier described nematode *Litylenchus crenatae* is known to induce similar symptoms on Japanese beech (*Fagus crenata* Blume) throughout Japan (Kanzaki et al. 2019). While it is clear that the nematode is a fundamental component of this pathosystem, there is still active debate regarding the precise mechanism of BLD symptom development, associated damage, and the potential role of fungal and/or bacterial symbionts in BLD (Burke et al. 2020; Ewing et al. 2021). Investigations of American beech buds during the dormant season have documented the presence of *Lcm* within the secondary interveinal regions of primordial leaves (Vieira et al. 2023). Nematodes found within these regions are responsible for a proliferation of cell division, resulting in marked increases in the layers of spongy and palisade mesophylls, abaxial and adaxial epidermides, and thickening of the tertiary and minor veins (Fletcher et al. 2023; Vieira et al. 2023). These changes induced within leaf primordia at the cellular level manifest as symptoms that are readily observable immediately following leaf flush in the spring, notably as discoloured bands of tissue (diffuse galls) within the interveinal regions of the leaf, stunted and crinkled leaf morphology, chlorosis and necrosis (Figure 1). The severity of these symptoms is proportional to the abundance of nematodes within the bud during the time of leaf development (Vieira

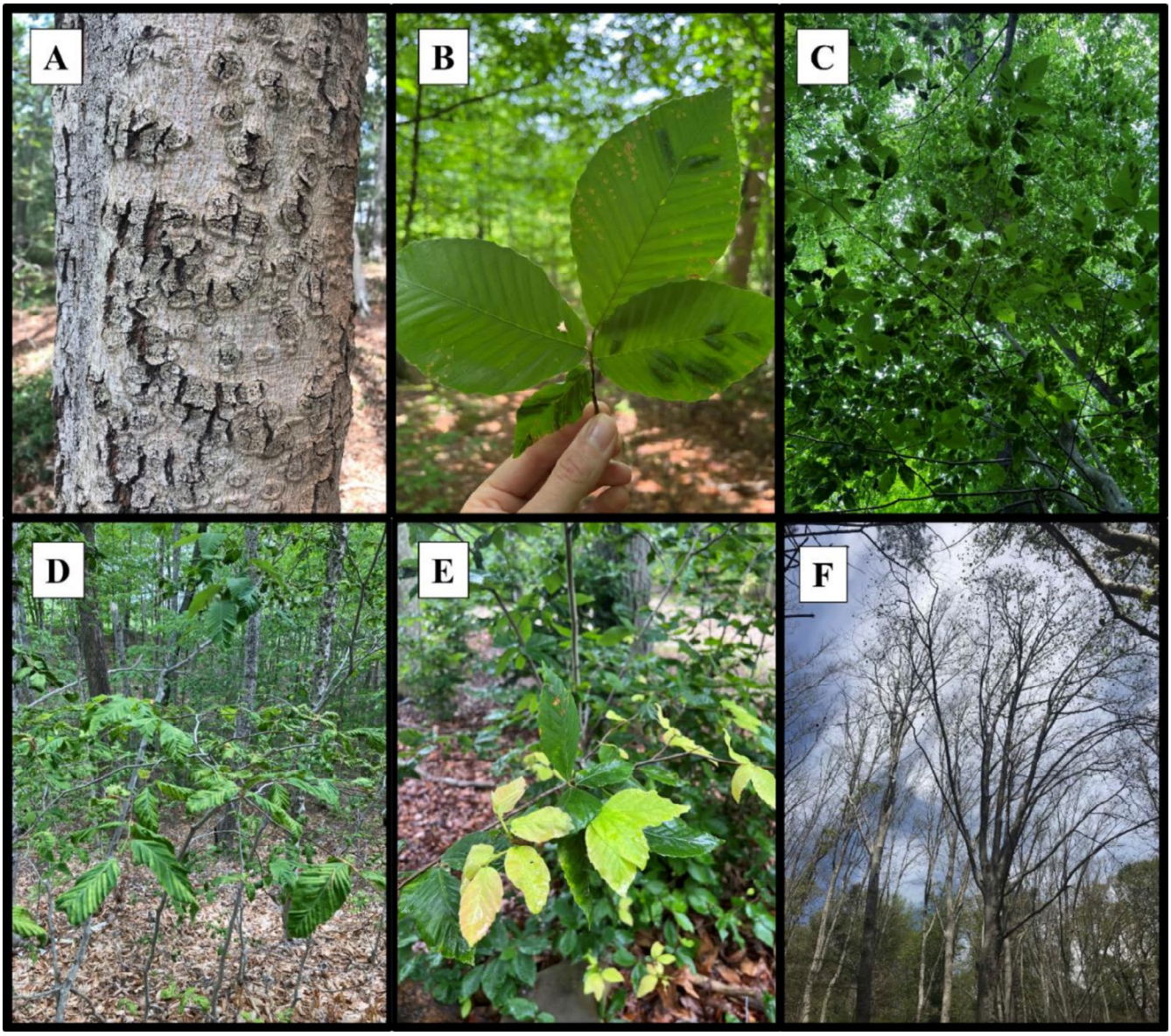

FIGURE 1 | Cankering caused by *Neonectria* fungi associated with beech bark disease expressed at a representative symptom severity across the three study sites (A). Mild banding symptoms on individual leaves associated with BLD among trees the low-severity site (B). Upward facing view of the canopy at the low-severity site, note the nonuniform banding symptoms and dense crown cover (C). Advanced crinkling leaf symptoms induced by BLD at the high-severity site (D). Production of second flush leaves at the high-severity site are easily identified by their shrunken size and light green appearance (E). Upward facing view of the beech canopy at the high severity site showing significantly reduced leaf are within BLD infested trees (F).

et al. 2023). When *Lcm* abundance reaches a critical threshold, buds will often fail to produce viable leaves and can abort from the branch entirely (McIntire and Vieira 2025). The observable symptoms of BLD also have measurable impacts on leaf functional traits, including elevated leaf water content and reduced specific leaf area, photosynthetic capacity and instantaneous water use efficiency (Fletcher et al. 2023; McIntire 2023). A natural consequence of these anatomical and physiological changes is an increased demand on carbon resources, and a reduction in non-structural carbohydrate (NSC) storage would therefore be expected, although this has not yet been thoroughly quantified in mature trees. Changes in carbon storage and flux due to BLD could also plausibly impact microbial communities associated with beech trees such as ectomycorrhizal (ECM) fungal communities (Bashian-Victoroff et al. 2023). Ectomycorrhizal fungi form mutualistic relationships with trees where trees provide photosynthetically derived carbon to the fungi in exchange for nutrients scavenged and transferred to the host tree by fungi (Smith and Read 2010). Different ECM fungi have varying carbon requirements based on their fungal traits such as their exploration types (i.e., mycelium production and foraging strategies) with contact exploration types having lower carbon requirements compared to long-distance exploration types that produce ample mycelium and forage far from tree roots (Agerer 2001; Peay et al. 2011). Shifts in the proportion of exploration types have been observed in other stressed systems (e.g., drought; Castaño et al. 2023). As BLD progresses, these physiological impacts may interfere with the tree's ability to allocate carbon effectively to ECM fungi, potentially altering these communities. Once a stand is infested with BLD, the symptom severity generally increases annually as the *Lcm* population continues to expand throughout the beech canopy, resulting in branch dieback and declines in overall crown density (Reed et al. 2022). Trees exhibiting marked reductions in crown density often produce a secondary flush of leaves in the early summer. However, while these second-flush leaves do not have outward symptoms of BLD and are functional, they are generally stunted, fewer in number and appear to lack the chlorophyl content of healthy primary leaves, thus only compensating for a small fraction of the total leaf area and photosynthetic capacity lost due to bud abortion.

In addition to BLD, another non-native disease, beech bark disease (BBD), has plagued American beech in the northeastern US for over a century (Cale et al. 2017). BBD is a disease complex initiated by the invasive felted beech scale insect, *Cryptococcus fagisuga* Lindinger, which feeds on phloem parenchyma of the tree bole and subsequent infestation by one or both of the putatively native fungal pathogens, *Neonectria faginata* (M.L. Lohman, A.M.J. Watson & Ayers) Castlebury & Rossman and *Neonectria ditissima* (Tul. & C. Tul.) Samuels & Rossman. BBD symptoms manifest as bark necrosis, often localised within cankers on the bole of infested trees, which have a range of outward presentations. While there is some tolerance and even resistance to BBD present in American beech populations, the majority of beech trees appear to be at least moderately to highly susceptible such that finding canker-free trees within New England can be a challenge in some sites (Calic et al. 2017; Leak 2006; Taylor et al. 2013). While many BBD-infested trees are in decline, the species has largely maintained its historical importance, at least in part due to the aggressive, highly shade tolerant beech regeneration via seed and vegetative root sprouting (Garnas et al. 2011). Much of the northeastern region is within the aftermath forest of BBD, yet beech remains abundant on the landscape (Bose et al. 2017; Houston 1975). Areas of localised bark necrosis can coalesce, leading to girdling of the bole and subsequent canopy mortality. More often, however, growth losses due to infestation lead to canopy decline, reduced carbon uptake, and a general weakening of the bole due to declines in structural carbon (sapwood) production and the accumulated bole defects, leading to higher rates of bole failure under high snow, ice or wind loads (Papaik et al. 2005). Despite the low vigour among BBD-infested trees, they can persist under high levels of cankering and mortality is frequently coupled with other contributing stressors, such as drought (Kasson and Livingston 2012).

While BLD poses a significant threat to all American beech, accelerated decline among trees within the BBD aftermath forests is likely due to the compounding nature of physiological stress. As an effective pre-leaf out defoliator, BLD has no known direct impacts on the structural integrity of beech trees. Instead, the mechanism leading to mortality is thought to be rooted in carbon starvation, where the depletion of non-structural carbohydrates (NSC) following years of chronic BLD, or combined BLD and BBD infestation, renders trees incapable of maintaining growth and the metabolic processes necessary for survival (Mcdowell and Sevanto 2010; Plotkin et al. 2021; Wiley et al. 2013).

Based on current understanding of these interacting diseases, we outline four non-exclusive mechanisms that are expected to influence NSC dynamics and growth in affected trees. These mechanisms serve as a conceptual framework for interpreting early physiological responses rather than hypotheses directly tested within the scope of this study. Specifically, we expect NSC depletion to arise from the following processes: (1) reduced leaf area due to bud abortion and/or canopy dieback, which limits net carbon assimilation; (2) reduced photosynthetic capacity in residual leaves symptomatic for BLD; (3) reduced photosynthetic capacity among second-flush leaves formed after bud abortion; and (4) increased carbon demand associated with wound responses in trees concurrently infested with BBD and BLD.

To examine how these predicted mechanisms influence tree physiology under field conditions, we focused on American beech growing in forests where BLD occurs alongside chronic BBD infestation, a combination that reflects the typical stress environment across much of the northeastern range. Within this setting, our objective was to determine how variation in BLD severity corresponds to changes in NSC storage, radial growth, and ECM fungal communities. We measured woody diameter increment, NSC content across multiple tissue types (bole, twigs and roots) and ECM communities in three natural stands of American beech that differed in BLD symptom severity while maintaining similar levels of bole cankering associated with BBD. Our work aimed to address the compounded stress imposed by both BLD and BBD, leveraging a well-documented timeline of BLD invasion to evaluate how early physiological disruption may contribute to longer term declines in American beech.

2 | Materials and Methods

2.1 | Study Sites

Three field sites were selected across a gradient of BLD severity from a subset of plots within the US Forest Service's long-term monitoring plot network (Figure 2). These plots have been measured annually in Maine since 2021, the first year BLD was detected in the state. A detailed description of the plot measurement protocol can be found in Reed et al. (2022). Briefly, all mature trees (> 12.7 cm diameter at breast height (DBH), 1.3 m above ground level) are measured within a circular 0.04-ha fixed plot (11.3 m radius). Measurements consist of tree DBH (cm) and ocular estimates of crown density (%) and crown dieback (%) according to (Schomaker et al. 2007). Additionally, ratings of BLD symptoms are segmented into three categories: percentage of healthy asymptomatic leaves, BLD-symptomatic leaves exhibiting typical banding associated with mild infestations (Figure 1B), and BLD-symptomatic leaves exhibiting advanced crinkling and necrosis associated with more severe infestations (Figure 1D). As the different symptom types can occur simultaneously within the crown, percentages for each category are assigned as a whole-crown assessment, with the three proportions summing to the total crown foliage. These symptom observations are subdivided into five bins corresponding to 0% (1), 1%–25% (2), 25%–50% (3), 50%–75% (4) and 75%–100% (5). An overall BLD severity index is calculated as the sum of the banded and crinkled leaf ratings, with site average BLD severity reported in Table 1. A rating of BBD symptom severity is assessed according to the density of cankers on the main bole using an index value ranging from 0 to 5, where 0 corresponds to no observable symptoms and 5 is a severe infestation (see BLD long-term monitoring plot protocol in the Supplemental Data).

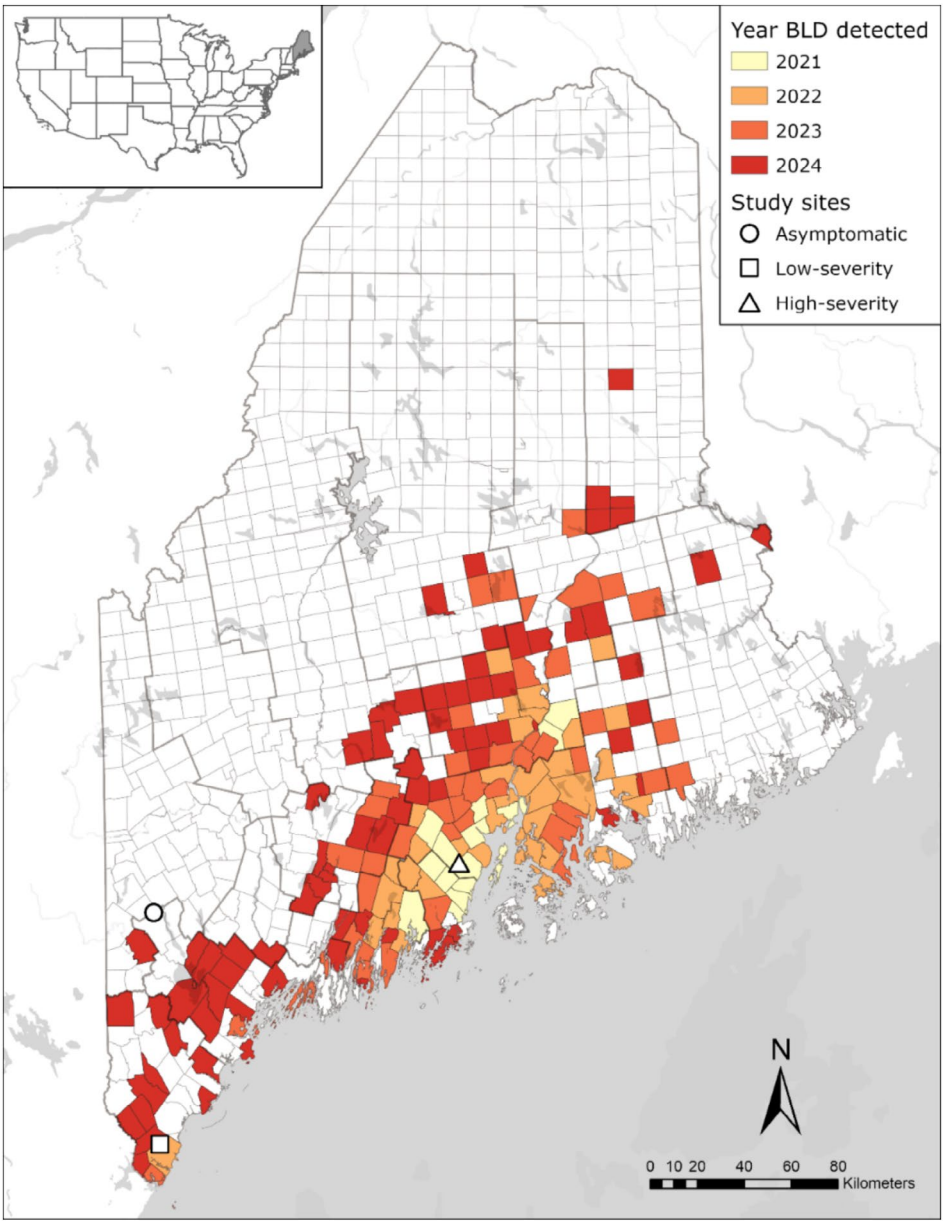

FIGURE 2 | Map showing the state of Maine with confirmed detections of BLD by municipality for 2021–2024. The locations of asymptomatic, low-severity and high-severity stands are denoted by shape markers.

TABLE 1 | Stand characteristics. Mean diameter at breast height (DBH; ±SD), trees per hectare (TPHA) and total basal area (BA) estimated from 0.04 ha fixed plots. Mean BLD severity is an index value that incorporates the total observed leaf symptoms within the crown, while the mean BBD severity is an index value of canker symptoms observed on the main bole.

Site	Time since BLD infestation	DBH (cm)	TPHA	Total BA ($m^2 ha^{-1}$)	Beech BA (%)	BLD severity[a]	BBD severity[a]
Asymptomatic	N/A	19.8 ± 4.6	469	22.5	70.0	0.0	3.4
Low-severity	1–2 years	24.7 ± 5.6	593	33.4	82.7	2.4	3.2
High-severity	3+ years	23.1 ± 6.1	544	36.0	63.2	7.4	3.7

[a]See Supporting Information for detailed protocol of the BLD long-term monitoring plot measurements.

A low severity site was selected at Mt. Agamenticus (York, ME), where BLD had been documented on a single tree in 2022, 1 year prior to this study. In 2023, all beech trees within the plot exhibited banded leaves associated with a mild BLD infestation, in which the average banded leaf symptoms were expressed in only 1%–10% of the crown in the year of sampling. A plot on private property in Lincolnville, ME was selected as the high-severity site, as this site was the first detection of BLD in the state and is known to have been infested for at least 3 years. Average banded leaf symptoms in the crown were < 25%, though heavy leaf symptoms associated with crinkled and stunted leaves were in the range of 50%–75% across all mature trees, accompanied by bud abortion and significantly reduced crown density throughout the stand. Finally, a control plot was selected at the Highland Research Forest (Bridgton, ME) where BLD symptoms have not been documented. Photos of representative stands conditions and disease expression are shown in Figure 2. While the three sites had contrasting levels of BLD severity, other site factors were carefully considered to select plots that had comparable tree size metrics, stand composition and cankering associated with BBD (Table 1). A one-way ANOVA showed a modest difference in DBH among sites ($p = 0.022$), driven by several larger trees at the low-severity site compared to the control site. Control trees ranged from 13.0 to 26.2 cm, low-severity trees ranged from 17.4 to 39.6 cm, and high-severity trees ranged from 13.2 to 35.3 cm. These ranges indicate broadly comparable tree sizes across plots and thus we do not anticipate size variation to have an outsized influence on the physiological or growth responses evaluated in this study.

To ensure that climatic differences did not confound our interpretation of site-level responses, we evaluated the previous 30 years of monthly temperature and precipitation data for each site using climate normals at 4-km resolution (PRISM Climate Group 2024). Long-term mean annual temperatures ranged narrowly from 6.6 C to 8.8 C across sites, and mean annual precipitation ranged from 1263 to 1316 mm $years^{-1}$, with similarly comparable growing-season conditions (May–September). These values indicate that all plots occupy the same regional climate envelope (Appendix A, Figure A1). We also calculated annual and growing-season anomalies across the full 30-year record and found that the sites experienced coordinated interannual variability, including shared drought events such as the well-documented 2001 statewide drought (Kasson and Livingston 2012), and a consistent pattern of warmer-than-average temperatures during the 4 years preceding sampling (Appendix A, Figure A2). No site exhibited unique or site-specific climatic stressors. These observations validate that the study plots are climatically comparable and that recent conditions are unlikely to be primary drivers of observed differences in our response variables.

2.2 | NSC Tissue Collection and Processing

All three plots were sampled between November 14 and 16, 2023. A total of 20 mature trees were sampled within each plot, focusing on the larger diameter co-dominant individuals. Two bark and cambium tissue samples were collected on opposite sides of the main bole at breast height using a 1.5 cm diameter cork borer. Similarly, a cork borer was used to collect two bark and cambium tissue samples from coarse primary roots within 1 m of the trunk. Twig samples ranging from 10 to 50 cm in length were collected using a combination of pole pruners, climbing, and shotgun sampling with 12-gauge steel buckshot. All twigs were taken from the lower portion of the mature crown from branches approximately 8–15 m above ground level, corresponding to the lower crown zone for American beech within the diameter range sampled. From the twig samples, at least six live buds were harvested for conducting nematode counts. Each tissue sample was placed in a separate plastic zip-lock bag and stored on ice inside a cooler while in the field. Upon returning from the field, all bud samples were shipped overnight on ice to the Bartlett Tree Research Laboratories in Charlotte, NC, USA. There, buds for nematode quantification were stored at 4°C until processing within 1 week, as described in a subsequent section. The other buds were immediately stored at −20°C for later processing. For processing, bole, root and twig samples were removed from the freezer, placed directly into a mortar and pestle containing liquid N, and hand-ground into a powder. Approximately 20 mg tissue (±1 mg) were then weighed, placed into individual 1.5 mL microtubes, and stored at −20°C until shipped. Samples were shipped overnight on dry ice on 8 February 2024 to the Plant Pathology Laboratory at The Morton Arboretum in Lisle, IL, USA and arrived on 9 February 2024 where tissue was stored at −30°C prior to NSC extraction and quantification.

2.3 | Dendrochronology

A 5.15 mm increment borer was used to extract a single core at breast height from each tree extending to the pith. Cores were stored in plastic tubes in the field, then air dried for

72 h prior to mounting. Cores were polished with sandpaper (120–800-grit), then scanned on a flatbed scanner at 1600 dpi (Epson Expression 12000XL; Seiko Epson Corporation, Nagano, Japan). Digital core images were used for ring width measurements to a precision of 0.001 mm in CooRecorder v9.8.4 (Maxwell and Larsson 2021). Cross dating was performed with the xDateR shiny app within the dplR package in R (Bunn 2008, 2010). Raw ring width measurements were converted to basal area increment, where diameter inside bark was estimated using a generalised hardwood equation (Miles and Smith 2009).

2.4 | NSC Analysis

The extraction and quantification of NSCs followed the phenol-sulfuric acid method described by Hill et al. (2012) and Rigsby et al. (2019) with a few minor adjustments to aid in throughput. All standards and phenol were purchased from Sigma-Aldrich (St. Louis, MO, USA) and all solvents and acids were purchased from Fisher Scientific (Hampton, NH, USA). Sugars were first quantitatively extracted three times (1 mL each) in 12:5:3 (v:v:v) methanol:chloroform:water and 2.4 mL of the combined 20,000*g* supernatants were mixed with 1.2 mL water. Tubes containing extracts were then centrifuged at 3000*g* to aid in phase separation, and 160 μL of the top phase was removed and diluted in 800 μL water. Sugar extract from each sample was then pipetted into two separate 1.5 mL tubes, each containing 300 μL extract to obtain a test and control for each sample. All control tubes received 10 μL water and all test tubes received 10 μL 100% phenol and were vortexed. Test and control tubes for each sample were then pipetted (46 μL) in duplicate into the wells of a standard microplate, followed by 154 μL concentrated sulfuric acid. Each plate was incubated at room temperature for approximately 5 min and then the absorbance at 490 nm was recorded on a microplate reader (Synergy HTX, Biotek, Winooski, VT, USA). A standard curve of glucose was carried through the entire procedure, and each plate included a standard curve. The absorbance of control reactions was subtracted from the absorbance of test reactions to account for background interference and sugar content is expressed as mg glucose equivalents per g tissue ($mg\,g^{-1}$).

Starch was extracted from the dried (at 50°C for 48 h) tissue remaining from the sugar extraction by incubating tissue with 1 mL 35% perchloric acid at room temperature for 1 h. After incubation, 80 μL of the 20,000*g* supernatants were recovered and diluted in 800 μL water. These extracts were then subjected to the same phenol-sulfuric acid quantification procedure as the sugar extracts. A sample was transferred to two separate tubes containing 300 μL for tests (10 μL phenol) and controls (10 μL water), vortexed and transferred (46 μL) to the wells of a microplate in duplicate, followed by the addition of 154 μL sulfuric acid, and then recording of the absorbance at 490 nm after a 5-min incubation at room temperature. As with sugars, a standard curve (using rice starch) was carried through the entire procedure for each plate. Background absorbance was accounted for as before, and starch content is expressed as mg starch equivalents per g tissue ($mg\,g^{-1}$).

2.5 | Quantification of Nematode Populations

For each tree ($N = 60$, 20 per site) six buds from each twig sample were placed in a 15 mL conical tube in the field and shipped with ice packs overnight to a diagnostic lab. From each sample, buds were first weighed and then bud sheaths were opened with forceps. Opened buds were submerged in 10 mL of distilled water in 60 mm diameter petri dishes and held in the dark for 24 h. Nematodes were then counted under a dissecting microscope using a mounted light below the petri dish. Counts were separated based on vermiform or worm stage (immatures and adults) and eggs extracted from buds. The extracted nematodes in each stage and total (vermiform + eggs) counts were standardised by mass of buds used in the extraction.

2.6 | Analysis of Fine Roots

Fine roots were collected approximately 10 cm deep and parallel to the randomly selected, coarse lateral root sampled for NSC analyses using a hand trowel and hand rake. Approximately one clean quart-sized Ziploc bag (~950 cm^3) was filled with roots and all adhering soil. Roots were rinsed several times in running tap water to remove adhering soil in the lab prior to further processing. Using a stereomicroscope, ectomycorrhizal (ECM) root tips were separated by morphotype based on colour, shape and branching patterns (Agerer 2006). Briefly, for each individual tree, one representative per morphotype was blotted dry and placed in 25 μL of extraction buffer from an Extract-N-Amp buffer (Vandepol et al. 2020). Molecular methods were as follows: according to (Karlsen-Ayala et al. 2023) with minor modifications to the PCR master mix solution. The master mix contained 3 μL GoTaq MDx buffer (Promega, Madison, WI, USA), 1 μL $MgCl_2$, 0.3 μL dNTPs, 0.3 μL ITS1F primer (Gardes and Bruns 1993) and 0.3 μL ITS4 primer (Vilgalys and Hester 1990), 0.1 μL taq polymerase, 0.12 μL BSA, 2 μL DNA and 7.88 μL of molecular grade water. Roots tips were Sanger sequenced at Yale University Keck DNA Sequencing Core in New Haven, CT, USA.

2.7 | Statistical Analyses

While each BLD severity class is represented by a single forest plot, our experimental design prioritised a high degree of within-stand replication ($n = 20$ trees per site) coupled with a rigorous assessment of plots within the BLD long-term monitoring network (218 total plots) to mitigate issues of spatial replication and ensure similar structural characteristics but contrasting disease duration and severity. Through this approach we assert that our response metrics are predominantly driven by BLD but recognise that underlying environmental heterogeneity can also influence tree response between sites. Given logistical constraints (i.e., the high cost of NSC analysis and the need to include reasonably large number of replicate trees within each site, to adequately create site-level reference chronologies) our design only includes tree and not site level replication across severity categories. While not ideal, we were able to compare growth rates prior to the arrival BLD and did not detect any site-level patterns

in growth, strengthening our interpretation that among-site differences in our response variables are primarily attributable to BLD.

NSC contents were analysed via a two-way ANOVA with NSC (sugar, starch or total) as the response variable and site-level BLD severity and tissue type (root, twig and bole) as predictor variables. Post hoc Tukey tests were used to separate BLD severity × tissue type means. Statistical analysis of NSCs was performed in R (R Core Team 2025).

To assess the influence of BLD infestation on tree growth we defined a pre- and post-outbreak period for our sites based on the initial observation of disease symptoms within the long-term monitoring plots. For the low-severity site, symptoms were first observed in 2022; therefore, the post-outbreak period included 2 years of growth (2022 and 2023). For the high-severity sites, symptoms were first observed in 2021; therefore, the post-outbreak period included 3 years of growth (2021, 2022 and 2023). In order to establish a breakpoint for comparison within the asymptomatic site, we elected to use the same 3-year period as the high-severity site (2021, 2022 and 2023). The pre-outbreak period across all sites was defined as the 10 years immediately prior to BLD infestation, such that the low-severity site considered 2012–2021, while the other two sites considered the period of 2011–2022. The mean basal area increment (BAI) was calculated for each tree with respect to the defined pre- and post-outbreak periods; then the percent change was expressed as:

$$\Delta\text{BAI} = \frac{\left[\text{BAI}_{\text{post}} - \text{BAI}_{\text{pre}}\right]}{\text{BAI}_{\text{pre}}} \quad (1)$$

where ΔBAI is the change in basal area increment, BAI_{post} is the mean post-outbreak basal area increment, and BAI_{pre} is the mean pre-outbreak basal area increment. Differences in site level ΔBAI were assessed using one-way ANOVA, followed by a Post hoc Tukey test to evaluate any significant differences between sites ($\alpha = 0.05$).

For nematode quantification, the abundance of vermiform, egg and total *Lcm* g^{-1} of bud tissue were each $\log(x+1)$ transformed to normalise variance prior to conducting an analysis of variance where *Lcm* g^{-1} was the response variable and site BLD severity condition (i.e., site) was the fixed effect. Means were separated with a Tukey's HSD post hoc test ($\alpha = 0.05$).

ECM sequence quality and trimming was performed using Geneious v. 2022.0.1. Sequences were grouped into contigs using de novo assembly tool in align/assemble. Non-fungal reads were removed prior to community analyses. Fungal community analyses were performed using the vegan package in R version 2023.03.0. To visualise fungal community composition based on BLD severity, we converted the matrix to presence/absence and used *vegdist* function with the Bray–Curtis dissimilarity matrix. Fungal community composition was visualised using a principal coordinate analysis (PCoA). To assess if differences in the ECM community were attributed to BLD severity, we used a nonparametric permutational multivariate analysis (PERMANOVA) with the *adonis2* function and then used the *betadisper* function to test for differences in multivariate dispersion. Alpha diversity measurements were assessed using the *alphaDiversity* function in the *otuSummary* package.

Principal component analysis (PCA) was used to evaluate the association between health metrics collected on individual trees within the long-term monitoring plots with the NSC, BAI, and ECM data products described above. We identified health metrics with anticipated influences on tree carbon balance; specifically, these included estimates of crown density, crown dieback, and two levels of BLD symptom expression: banded leaves (mild/moderate condition) and crinkled leaves (severe condition). We incorporated total NSC values for each measured tissue type, along with ΔBAI and estimates of ECM richness. Data were standardised using a *z*-score transformation, and PCA was conducted using the *prcomp* function within the ggfortify R package (Tang et al. 2016).

3 | Results

3.1 | Non-Structural Carbohydrates

Sugar content of beech trees was significantly impacted by site-level symptom severity ($F_{2,171} = 6.2$, $p = 0.002$) but not by tissue type ($F_{2,171} = 1.5$, $p = 0.223$). However, there was a significant symptom severity × tissue type interaction ($F_{4,171} = 2.7$, $p = 0.032$) on sugar content. Generally, the sugar content of the root and trunk tissue of asymptomatic trees was greatest and sugar content of the roots from trees at the low-severity site was lowest. The remaining tissue types from trees across the symptom spectrum were not statistically distinguishable (Figure 3A). For starch contents, there was also a significant effect of site-level symptom severity ($F_{2,171} = 93.1$, $p < 0.001$) and tissue type ($F_{2,171} = 3.7$, $p = 0.027$), but there was no interactive effect between these predictors ($F_{4,171} = 2.0$, $p = 0.098$). Regardless of tissue type, starch content was always highest in asymptomatic trees and statistically distinguishable from trees symptomatic of BLD regardless of symptom severity (Figure 3B). Total NSC content (sugars + starch) was significantly impacted by site-level severity ($F_{2,171} = 65.6$, $p < 0.001$) and tissue type ($F_{2,171} = 4.258$, $p = 0.016$) and there was a significant site × tissue interactive effect ($F_{4,171} = 2.7$, $p = 0.033$). As with starch, total NSC content was always statistically greatest in beech tissues from the asymptomatic site, and this was always distinguishable from the sites with visual BLD symptoms. Full statistical results of the NSC data are shown in Appendix Tables A1 and A2.

3.2 | Dendrochronology

A tree ring master chronology was generated for each of the three sites (Figure 4). Crossdating yielded interseries correlation values of 0.322, 0.372 and 0.365 for the asymptomatic, low-severity and high-severity stands, respectively. Despite our effort to standardise sampling across trees of a similar diameter (Table 1), we noted considerable differences in the estimated age and year of establishment for each site. The average series length of cores sampled within the asymptomatic site was 64 years, with the earliest measurement dating to 1948, making it the youngest stand among those sampled in the study. The low-severity stand was

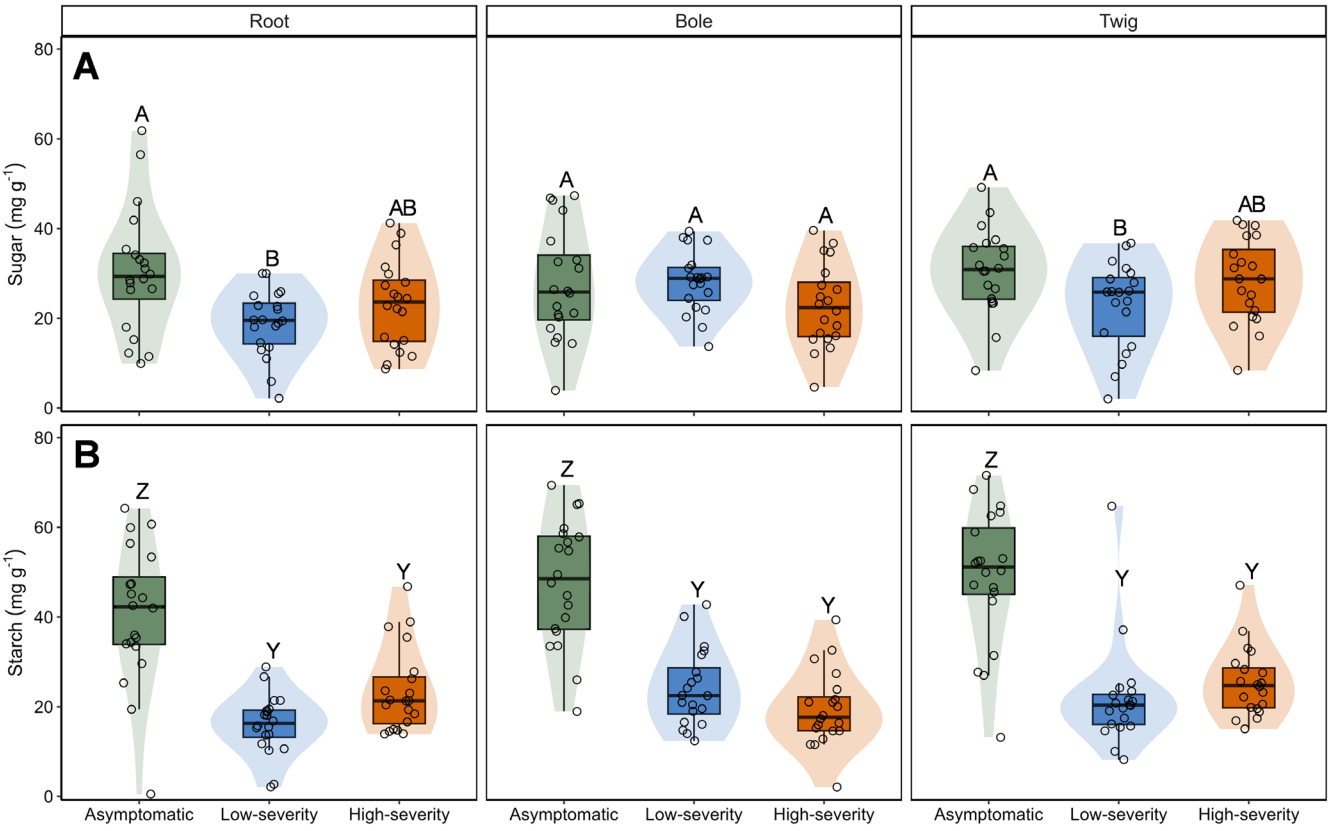

FIGURE 3 | Boxplots of sugar (A) and starch (B) content (mg g^{-1}) of twig, root and trunk tissue of beech trees at sites with low and high beech leaf disease symptom severity as well as at the site with asymptomatic beech. Boxplots represent the median of the data and the lower and upper quartiles (25% and 75%); whiskers extend to 1.5 times the interquartile range. The shaded region is the continuous density distribution and open circles denote individual tree replicates. Statistical differences are indicated by different letters between symptom categories (Tukey post hoc analysis, $p < 0.05$).

determined to be our oldest site, with an average series length of 118 years and an estimated establishment dating to 1875. Finally, the high-severity site had an average series length of 77 years with an estimated establishment of 1934. All sites exhibited similar rates of growth prior to BLD arrival: mean 10-year pre-disease BAI was 5.0 cm^2 (SD ± 1.3) the asymptomatic site, 5.9 cm^2 (SD ± 1.2) at the low-severity site and 5.6 cm^2 (SD ± 1.3) at the high-severity site, with no significant differences among stands (ANOVA $p = 0.286$). BAI differed significantly between sites in the time following the arrival of BLD symptoms ($F_{2,52} = 18.6$, $p < 0.001$) (Figure 5). Comparison of post-outbreak BAI relative to the previous 10 years indicated that growth declined at the high-severity site 47.6% (SE ± 4.2). Interestingly, BAI slightly increased at the low-severity site by 5.9% (SE ± 7.9), though it should also be noted that growth at this site was the most variable, with nine out of the 20 trees exhibiting negative growth rates with respect to the pre-outbreak period. BAI within the asymptomatic site had a relative decline of 26.0% (SE ± 5.6) when comparing the most recent 3 years of growth to the previous 10 years, though this decline cannot be attributable to BLD. Full statistical results of the tree ring data is shown in Appendix Tables A3 and A4.

3.3 | Nematode Abundance

We detected significant differences in nematode populations between sites with respect to vermiform *Lcm*, *Lcm* eggs, and total *Lcm* (Table 2). The vermiform and total amount of *Lcm* did not statistically differ (Tukey post hoc analysis, $p > 0.05$) between the low-severity (17,935.9 g^{-1}) and high-severity sites (17,682.8 g^{-1}). However, the low-severity site was found to have 119% more Lcm eggs than the high-severity site (Tukey post hoc analysis, $p < 0.05$). We detected low levels of vermiform *Lcm* (0.3 g^{-1}) and *Lcm* eggs (0.2 g^{-1}) within the asymptomatic site. Notably, this corresponded to a single bud measured to have 5.4 vermiform *Lcm* g^{-1} and one other bud with 4.7 *Lcm* eggs g^{-1}, while the other 18 measured buds did not present nematodes. Alternatively, 100% of the buds within the low- and high-severity sites contained *Lcm*. Mean bud mass was measured at 0.498 g (±0.183), 0.429 g (±0.190) and 0.3521 g (±0.131) at the asymptomatic, low-severity and high-severity stand, respectively.

3.4 | Fine Roots

After quality filtering, a total of 159 sequences grouped into 44 contigs. A range of 1–6 operational taxonomic units (OTU) was recovered from each tree, with an average of 2.69 OTUs per sample. A total of 15 ectomycorrhizal lineages were found from root tips (Appendix Table A5). There were 12 lineages recovered from asymptomatic trees, 11 from low-severity trees, and 10 from high-severity trees. Overall, the more frequent OTU lineages recovered from trees across all symptom groups were

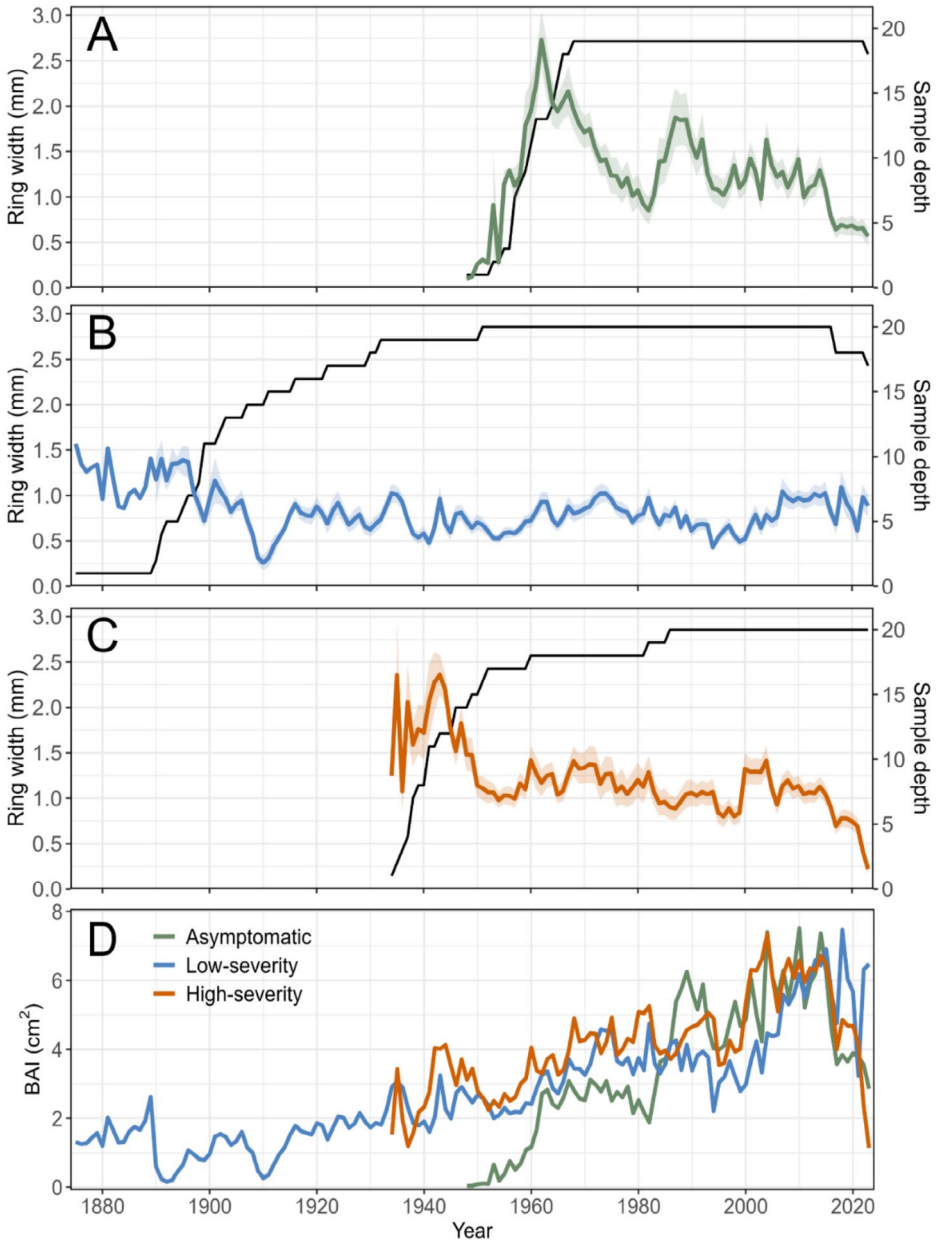

FIGURE 4 | American beech tree ring chronologies. Raw ring width means are shown for the asymptomatic (A), low-severity (B) and high-severity (C) stands, where the shaded region denotes ± standard error and sample depth is indicated by black lines on the secondary axes. (D) Comparisons of basal area increments (BAI) for each stand.

the/russula-lactarius/tomentella-thelephora, and/cortinarius lineages (Appendix Figure A3). The root tip fungal community was significantly different among site-level symptom severity (adonis2 $R^2 = 0.05$, $F_{2,55} = 1.6$, $p = 0.02$), and the multivariate dispersion was not significantly different between site-level symptom severity ($p = 0.84$). Proportion of long-distance versus short-distance exploration types and alpha diversity measurements were not significantly different between site-level symptom severity.

3.5 | Multivariate Analyses

Using PCA incorporating health metrics measured within the BLD long-term monitoring plots with tree-level NSC and BAI data yielded a biplot that explained 64.3% of the total variation within the first two principal components, with PC1 accounting for 43.7% and PC2 accounting for 20.7% (Figure 6). Examination of the scatterplot for PC1 and PC2 shows discrete clustering of trees with respect to disease severity and the different sites. ECM richness had the weakest association of any variable and was approximately parallel along PC1 positive loading. Negative loadings along PC1 corresponded to elevated values of crown dieback and were strongly associated with observed foliar symptoms of BLD, with clustering of trees experiencing a high severity of infection. Positive loadings within both PC1 and PC2 included metrics of total NSC (sugar + starch) within all tissue types (bole, root and twig) and were most strongly associated with the clustering of asymptomatic trees. The proportion of healthy leaves was positively associated with elevated crown density along PC1 and approximately inverse to metrics of crown density and

crinkled leaf symptomology. The clustering of trees within the low-severity site occupies an intermediate space on the biplot with respect to BLD symptom expression, associated with higher levels of growth but reduced levels of total NSCs, with some overlap among asymptomatic trees.

4 | Discussion

Interpreting the physiological and ecological consequences of beech leaf disease requires consideration of both disease severity and the broader environmental context in which infestations occur. Although BLD symptom development is strongly associated with nematode abundance within developing buds (McIntire and Vieira 2025), additional environmental and historical factors may influence the severity and progression of disease impacts. Climatic legacies such as seasonal moisture deficits or temperature extremes can alter host carbon balance and may affect susceptibility to foliar pathogens. Soil properties, including moisture availability and nutrient status, may also interact with BLD by influencing host vigour and belowground carbon allocation. As the colonisation history of *Lcm* varies across the region, differences in the timing or rate of pathogen establishment may contribute to variation in symptom expression among sites. These factors were not the primary focus of this study, but acknowledging their potential influence provides important context for interpreting site level differences in growth, NSC storage and ECM community composition. Within this broader framework, the patterns we observed across stands of differing BLD severity offer insight into how early physiological disruption may precede longer term declines in carbon balance and forest health. We recognise that the absence of site-level replication limits the generality of these findings, and our interpretations therefore focus on the physiological patterns expressed within the sampled stands.

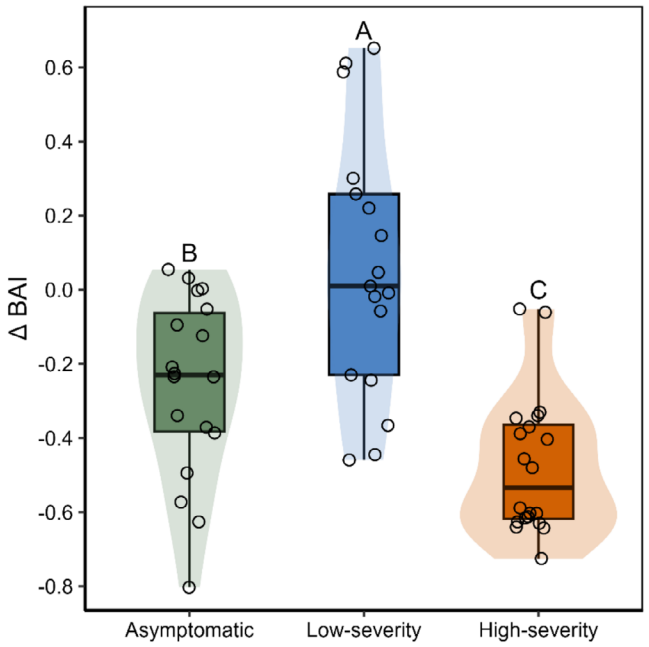

FIGURE 5 | Proportional change in post-BLD infestation basal area increment with respect to the previous 10 years of growth (ΔBAI). Boxplots represent the median of the data and the lower and upper quartiles (25% and 75%), whiskers extend to 1.5 times the interquartile range. The shaded region is the continuous density distribution and open circles denote individual tree replicates ($n = 20$). Statistical differences are indicated by different letters between symptom categories (Tukey post hoc analysis, $p < 0.05$).

We detected significantly lower NSC content, particularly in the starch component, in both the low- and high-severity BLD-infested stands with respect to the asymptomatic stand (Figure 3). This finding was consistent across all three tissue pools (root, bole and twig) measured at the beginning of the winter dormancy period. Previous work has documented seasonal dynamics of NSC within the bole tissue of hardwood tree species in the northeastern US, including American beech, which has shown to maintain higher levels of sugar in the dormant season relative to starch across multiple years (Richardson et al. 2012). This relationship was consistent for our symptomatic sites, where bole sugar was measured to be 16.5% and 17.4% higher than starch among the low-severity and high-severity trees, respectively. Interestingly, while bole sugar content was not statistically significant between our three study sites, starch content in the asymptomatic stand was 74.1% higher than sugar content. The drivers of starch, and in turn total NSC, depletion among the BLD-infested stands may be influenced by multiple factors resulting from disease. Trees within the low- and high-severity sites possess a carbon sink that is not present within the asymptomatic stand via an investment into symptomatic leaves. Through nematode-induced cellular division which results in a thickening of the mesophyll and epidermis (Fletcher et al. 2023; Vieira et al. 2023), the production of symptomatic leaves comes at an energetic cost to the tree. Though symptomatic leaves do photosynthesize they are much less efficient (McIntire 2023). Depending on infestation severity and timing on early

TABLE 2 | Average number of extracted *Lcm* nematodes per gram of bud tissue from each of the three sampling locations. Vermiform nematodes were motile juveniles and adult *Lcm*. Total *Lcm* g^{-1} of bud tissue included all motile and egg staged counts. Prior to ANOVA analysis, counts were log $(x+1)$ transformed to normalise the variance. Differences in letters within *Lcm* groups were found to be significantly different between stands (Tukey's HSD post hoc means separation test).

Site	*N*	*Lcm* (vermiform) g^{-1}	*Lcm* (eggs) g^{-1}	Total *Lcm* g^{-1}
Asymptomatic	20	0.3 (0.3) b	0.2 (0.2) c	0.5 (0.3) b
Low-severity	20	11,669.2 (2262.1) a	6266.6 (1375.1) a	17,935.9 (2930.6) a
High-severity	20	14,816.8 (2130.9) a	2866.1 (1108.4) b	17,682.8 (2556.5) a
p-value		< 0.0001	< 0.0001	0.0001

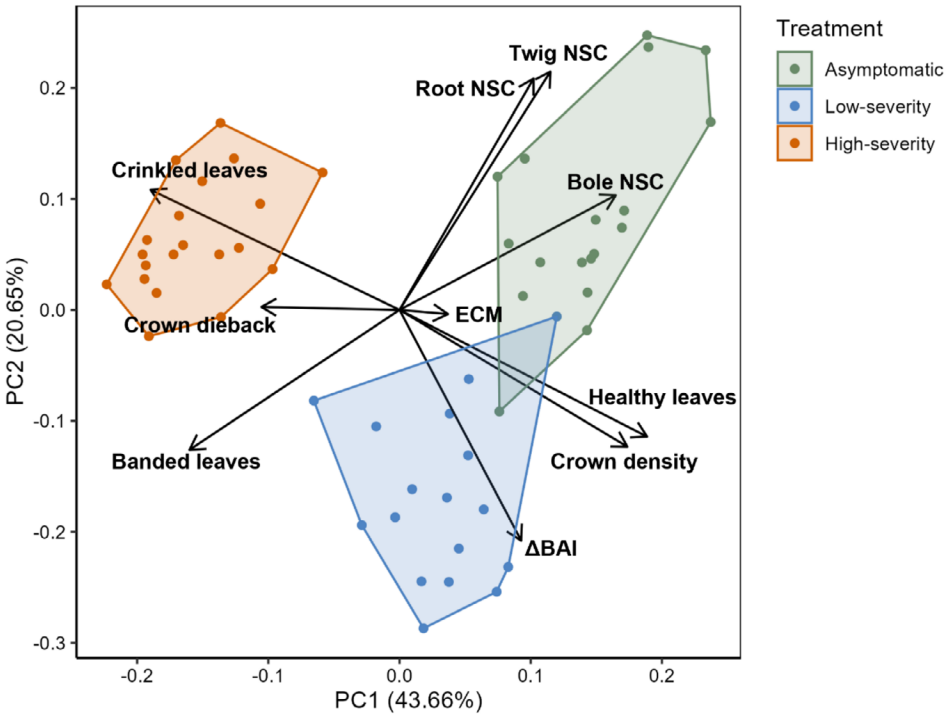

FIGURE 6 | Principal component analysis (PCA) biplot of beech leaf disease impact metrics along PC axes 1 and 2. Points indicate individual tree replicates while colour groupings denote overall disease severity at the sites sampled in this study. Healthy leaves, banded leaves, and crinkled leaves correspond to observations of BLD symptom expression throughout the crown, measured annually along with crown density and crown dieback within the long-term monitoring plots. Root, twig and bole NSC correspond to total non-structural carbohydrate (sugar + starch) contents measured within the respective tissue pools. ΔBAI is the change in post-BLD infestation basal area increment with respect to the previous 10 years of growth. ECM is the richness of the ectomycorrhizal community associated with tree fine roots.

abscission, these leaves may even represent a net negative carbon investment, though calculating the precise quantity of that NSC investment is beyond the scope of this study. There were two additional factors unique to the high-severity site: a marked reduction in overall leaf density and the production of second flush foliage. Though second flush foliage was not directly quantified in this study, it has been shown to be the prevailing leaf type in stands with late stage BLD infestation (McIntire and Vieira 2025). The bud abortion associated with BLD mimics conditions that are representative of defoliated stands, which puts infested trees at a disadvantage in terms of photosynthetic capacity. The impacts of leaf loss have been modelled in forested ecosystems subjected to insect defoliation, indicating reductions of net canopy assimilation, net primary production, and tree carbon storage pools (Medvigy et al. 2012; Schaefer et al. 2010). Furthermore, the production of second-flush leaves act as a sink for mobile carbon that may otherwise be allocated to growth, defence, or storage. The degree to which beech trees depend on stored carbon to produce second-flush leaves warrants investigation, though at least one study has suggested that re-flush leaves of aspen (*Populus tremuloides*) draw little from root NSC polls but rely more heavily on current-year photosynthate for re-flush (Hart et al. 2024). The evident NSC depletion among BLD-infested trees may have long-term consequences for vegetative reproduction, as American beech is known to aggressively sprout via adventitious root buds. The propensity to resprout is a key factor facilitating the maintenance of beech relative abundance on the landscape despite the decades of dieback associated with BBD in the northeastern US (Garnas et al. 2011). Mast production is also crucial, both for beech regeneration and as a high protein food for wildlife (Jakubas et al. 2005), and will also likely be negatively affected. The degree to which carbon depletion due to BLD will negatively impact vegetative and/or seed production is not yet known, though declines in one or both seem likely. Federal assistance for chemical suppression (i.e., herbicide application) of American beech has recently been curtailed by the Natural Resources Conservation Service in the state of New Hampshire, citing the high degree of uncertainty regarding how BLD will influence future regeneration.

We also report contrasting responses to growth with respect to the duration of BLD infestation, such that the low-severity stand maintained a stable BAI compared to pre-infestation growth, while the high-severity stand experienced a decline in BAI associated with the onset of BLD that was unprecedented in this stand's chronology (Figures 4 and 5). The sustained BAI accretion within the low-severity stand may be attributed to the crown condition of BLD-infested trees, where at the time of sampling overall leaf density was similar to pre-infestation estimates and symptoms were primarily composed of mild banding. Interestingly, the low-severity trees appeared to be prioritising radial growth over NSC storage in the early stages of BLD infestation. This pattern suggests that the reduction in NSC at the low-severity site reflects disease-related carbon sinks rather than carbon limitation, since radial growth remains unaffected. Nematode-induced cell division within developing leaves likely contributes to this early draw on stored carbohydrates, and additional sinks such as the formation of second-flush leaves

following bud abortion may further increase carbon demand as symptoms progress. Although such proliferative tissue could, in principle, represent a host attempt to compartmentalise nematode activity, current evidence suggests that this response is largely nematode-driven and functions as an additional carbon sink rather than an effective defence (Vieira et al. 2023). Because American beech shows little evidence of natural resistance to BLD, induced defences may be weak or nonexistent, limiting the tree's ability to constrain these accumulating carbon costs in later stages of disease. Growth data from the high-severity stand supports a lagged response between the onset of BLD infestation and BAI reduction, where moderate BLD symptoms were first documented in 2021 and significant declines in BAI did not occur until 2022 and 2023, corresponding to a relative decline of 43.5% and 72.8%, respectively. While the asymptomatic stand offers a reference point for NSC storage pools, a time series of pre- and post-infestation NSC within sites experiencing BLD could further elucidate the coordination between carbon storage and growth. Due to the chronic nature of BLD, it is not anticipated that growth within declining beech stands will naturally recover to pre-infestation levels and ongoing long-term monitoring should be used to record the incidence of future mortality.

In addition to these growth patterns, we also observed differences in tree age among the three stands, despite their broadly comparable diameters. Part of this variation reflects sample depth, as a small number of older individuals extended the length of the chronology in the low-severity stand. Additionally, age–diameter decoupling is well documented for *Fagus grandifolia*, a highly shade-tolerant species capable of persisting for decades in the understory before canopy release and accelerated radial growth (Canham 1990). Although differences in site quality could also contribute to age variation, we did not evaluate site productivity directly, and the observed patterns are consistent with species-typical suppression and release dynamics rather than clear differences in site conditions. Consistent with this interpretation, mean basal area increment during the 10 years preceding BLD arrival did not differ among stands, indicating comparable recent growth histories prior to infestation. Moreover, current evidence indicates that susceptibility to BLD is more strongly associated with local nematode inoculum pressure than with tree age alone, suggesting that the age structure of our sampled trees is unlikely to drive the decline patterns documented in this study. Our observation of elevated BAI in the low-severity stand suggests that trees retain substantial functional leaf area and do not experience immediate growth suppression in early stage BLD infections.

A multivariate analysis using PCA reduced variables into fewer dimensions, allowing for the identification of patterns associated with BLD symptom expression and among the measured impact metrics (Figure 6). Interpretation of PC1 and PC2 revealed discrete clustering of trees associated with BLD symptom types (asymptomatic, low-severity, high-severity), such that trees subjected to low-severity infection (1–2 years) shared some characteristics of asymptomatic trees, as BLD can linger for several years before more damaging impacts are realised. The tight clustering of the high-severity trees suggests that symptom expression may reach an equilibrium at the later stages of BLD infection, where observable impacts of disease (foliar disease symptoms, crown deterioration) begin to coincide with physiological impairment (reductions in growth and NSC pools). Hence, knowledge obtained from long-term plot monitoring, such as BLD symptom onset and severity, may prove to be a useful tool for estimating the rate of stand decline if the impacts we have documented on carbon storage and allocation are broadly applicable. While we intentionally attempted to account for BBD between stands using a priori information of cankering symptoms, a spectrum of BBD severity, and host tolerance, may be an important covariate when assessing beech decline in the context of BLD at a regional scale.

Bud dissection provided additional insight into *Lcm* populations at the time of sampling. First, it should be noted that migration of *Lcm* from infested leaves into buds is presumed to begin in the late summer and continue through leaf senescence (Goraya et al. 2024; Reed et al. 2020), though beech are known to retain some foliage throughout the winter (Heberling and Muzika 2023). Therefore, nematode populations measured within the cohort of buds in November are indicative of symptoms that will present the following growing season. The mean number of vermiform *Lcm* exceeded 10,000 individuals g^{-1} within both low- and high-severity stands. This corresponded to a total abundance of vermiform *Lcm* that ranged from 340 to 16,750 individuals per bud at the low-severity stand and 743–11,698 individuals per bud at the high-severity stand. Comparing these vermiform *Lcm* counts to those conducted by Vieira et al. (2023) suggests an infestation level indicative of severe BLD that would be expected to produce leaf necrosis and bud abortion. Interestingly, we found a significantly higher abundance of *Lcm* eggs within the low-severity site relative to the high-severity stand. This could be attributed to a developmental lag induced by a difference in climate between the two sites, such that the low-severity site within the southern position of Maine may experience warmer average temperatures and more cumulative growing degree days which delayed egg hatching. The life cycle of *Lcm* is not entirely resolved and abiotic factors which influence reproduction and eclosion merit additional study. The minimal presence of *Lcm* found within the asymptomatic stand suggests a recent invasion of the nematode, which was not unexpected given the proximity to known BLD infestations and the rate of spread throughout Maine in recent years. To provide additional insight, we observed how the *Lcm* bud counts manifested symptoms while conducting remeasurements of the long-term monitoring plots in 2024. The asymptomatic stand did not exhibit any symptoms of BLD the following growing season, suggesting that the small nematode populations we measured (on only two individual trees) were not sufficient to present visible symptoms. The low-severity stand experienced a dramatic increase in symptom severity in 2024, where all trees were documented to have crowns dominated by second-flush leaves with clear signs of bud abortion and marked reductions in overall canopy density. Though this was anticipated on the basis of our nematode counts in the previous year, the magnitude of the change was extraordinary and illustrated the speed at which BLD can progress from year to year. The high-severity stand exhibited a similar proportion of symptomatic and second-flush leaves in 2024 compared to the previous year; however, no mortality has yet to be documented. While the year-to-year abundance of *Lcm* within infested stands is anticipated to amplify as the established population continues to reproduce within leaves and buds, nematodes can also

travel to susceptible trees from nearby inoculum sources. Thus, it is not possible to know what proportion of *Lcm* we measured within buds comes from within the host tree as opposed to vectored from elsewhere, while the mechanism of transmission and dispersal is still an active area of research.

Since ectomycorrhizal (ECM) fungi require photosynthetically derived carbon as an energy source (Smith and Read 2010), we hypothesized that disease severity might impact the community structure, diversity and richness of the ECM communities. Overall, the ECM communities between symptom class were significantly different ($p = 0.02$) and overall ECM lineage diversity was lowest in the high-severity symptom class (Figure S1), yet there were no significant differences in alpha diversity, or proportion of exploration types. This pattern is consistent with Bashian-Victoroff et al. (2023) where site location, not disease severity, had the strongest effects on ECM community composition. Since beech trees are obligately associated with ECM fungi, carbon is allocated to fungal partners even during periods of carbon limitation (i.e., fungal sporocarp before spring leaf out; Smith et al. 2007), potentially at the expense of growth and reproduction (Pringle 2016). Conversely, large carbon demand events like seedling masts can be accompanied by reductions in ECM fruiting sporocarps (Michaud et al. 2024). Mature trees support high diversity ECM communities (Bruns 1995), experience high ECM community turnover throughout the growing season (Taylor and Bruns 1999) and exhibit high inter-site variability. These factors make it difficult to detect changes in the ECM community structure directly related to BLD, at least in the short term (Druebert et al. 2009) or early in disease progression. Many experiments demonstrating negative consequences of carbon depletion on ECM community structure and function include seedling or young trees which are lower carbon dynamic systems with less ECM diversity and more sensitive to changes especially in the context of drought (Sapes et al. 2021) or defoliation (Saravesi et al. 2008). Nonetheless, prolonged BLD infestation coupled with increased tree mortality may shift this dynamic (Pec et al. 2020). Therefore, additional long-term studies using high-throughput sequencing across multiple sites and throughout the growing season are needed to monitor disease impact on ECM communities.

A decline or cessation of radial growth preceding NSC depletion induced by stress associated with drought and defoliation has been well documented in other field studies (Chuste et al. 2020; Oswald and Aubrey 2024; Piper et al. 2015; Puri et al. 2015). Global meta-analyses of defoliators indicate that canopy loss can lead to short-term growth declines, while reduction in carbon storage pools over the long-term can also lead to sustained growth reductions, indicating that NSC pools and growth are coordinated (Wang et al. 2021). Though it appears that NSC depletion is occurring within the BLD-infested stands measured here, neither stand has started to exhibit mortality and therefore total carbon starvation has yet to occur. BLD presents as a chronic infestation, where infested canopies progressively degrade year after year with no documented recovery to date. As crown density tends to decline annually as a function of BLD severity, it is not yet clear how long infested beech can perpetually re-flush foliage each spring before carbon reserves are exhausted and mortality occurs. As a highly shade tolerant species, beech is well-adapted to persist through long periods of low carbon assimilation. Observations of BLD within areas of the oldest-known infestations report that mature overstory trees succumb to disease within a period of 7 years, while reports of mortality among smaller diameter understory trees has been more common (Reed et al. 2022; Shepherd et al. 2025). Although BLD-associated mortality often emerges first in smaller diameter trees, presumably due to their limited carbon reserves and reduced buffering capacity, current evidence does not indicate that mature beech differ in their susceptibility to infection or in the expression of foliar symptoms. All size classes appear broadly vulnerable to BLD, and symptom severity in mature trees does not show a consistent relationship with DBH. Given this, and because our analyses focused on a relatively narrow size range of mature individuals, we do not expect size-related variation to bias the physiological or growth patterns reported here. Though it is also important to note that the incidence and severity of BBD in the western portion of the beech growing range is low (e.g., Ohio), such that areas initially infested with BLD do not experience the same level of compounding BLD/BBD pressure as in Maine. While the interaction between BLD and BBD is not presumed to be direct, we may expect that beech trees subjected to both diseases within aftermath forests to decline at an accelerated rate.

Our findings have direct management implications, as the observed lag between infection onset and mortality highlights a crucial window for intervention, offering important insights into disease progression and the timing of silvicultural or chemical control interventions. Coupling assessments of NSC with different management techniques may be useful for identifying a tipping point for the efficacy of treatments, such that infested trees may be unable to recover from disease after a threshold of carbohydrate depletion has been reached. Although our study focused exclusively on American beech, other species of beech (e.g., *F. sylvatica*) are known to be highly susceptible to BLD. European forests have not yet documented a BLD infestation, though European beech planted throughout North America represents an opportunity to further study disease impacts on growth and carbohydrate storage across different species.

5 | Conclusion

We leveraged a BLD long-term monitoring plot network to estimate impacts of disease severity on tree carbon storage and allocation towards radial growth. We found that BLD infestation can significantly reduce NSC content, particularly starch, in both low- and high-severity stands. This reduction is likely driven by a combination of factors, including increased carbon demand for symptomatic leaf production, reduced photosynthetic capacity due to leaf loss, the energetic cost of producing second-flush foliage and investment into wound response due to BBD co-infestations. Additionally, our findings suggest a complex relationship between BLD infestation, growth and NSC storage. While low-severity stands may temporarily maintain growth by prioritising radial growth over NSC storage, high-severity stands subjected to longer-term stress (3+ years) experience significant declines in both growth and NSC content. A continued depletion in carbon reserves is not metabolically sustainable, though we have yet to observe widespread mortality of trees in Maine attributable to BLD. These results highlight the

detrimental effects of BLD on tree health and the potential long-term consequences for forest ecosystems where American beech is a major component.

Author Contributions

Cameron D. McIntire, Andrew L. Loyd, Chad M. Rigsby and Jeff R. Garnas designed the study and prepared the manuscript. Cameron D. McIntire and Aaron Bergdahl facilitated site selection and permitting. Cameron D. McIntire, Andrew L. Loyd, Chad M. Rigsby, Elena Karlsen-Ayala, Aaron Bergdahl and Patrick Lemis conducted the field sampling. Caitlin Littlejohn and Andrew L. Loyd conducted the nematode counts. Chad M. Rigsby, Andrew L. Loyd and Caitlin Littlejohn conducted the analysis of non-structural carbohydrates. Elena Karlsen-Ayala conducted analysis of ectomycorrhiza communities. Patrick Lemis and Cameron D. McIntire conducted the dendrochronology analysis.

Acknowledgements

We are thankful for field assistance provided by Isabel Munck and Eli Greenleaf. The authors also thank Robert Bartlett Jr. for his continuing support and commitment to woody plant research and conservation. Dr. Meghan Midgley of the Center for Tree Science at The Morton Arboretum for use of the plate reader.

Funding

This research was funded by the F.A. Bartlett Tree Experts Company and USDA Forest Service Evaluation Monitoring grant 23-DG-11094200-468.

Conflicts of Interest

The authors declare no conflicts of interest.

Data Availability Statement

Data pertaining to this study is available at Zenodo: https://doi.org/10.5281/zenodo.15425231.

Peer Review

The peer review history for this article is available at https://www.webofscience.com/api/gateway/wos/peer-review/10.1111/efp.70068.

References

Agerer, R. 2001. "Exploration Types of Ectomycorrhizae: A Proposal to Classify Ectomycorrhizal Mycelial Systems According to Their Patterns of Differentiation and Putative Ecological Importance." *Mycorrhiza* 11: 107–114.

Agerer, R. 2006. "Fungal Relationships and Structural Identity of Their Ectomycorrhizae." *Mycological Progress* 5: 67–107.

Bashian-Victoroff, C., A. Brown, A. L. Loyd, S. R. Carrino-Kyker, and D. J. Burke. 2023. "Beech Leaf Disease Severity Affects Ectomycorrhizal Colonization and Fungal Taxa Composition." *Journal of Fungi* 9, no. 4: 497.

Bose, A. K., A. Weiskittel, and R. G. Wagner. 2017. "Occurrence, Pattern of Change, and Factors Associated With American Beech-Dominance in Stands of the Northeastern USA Forest." *Forest Ecology and Management* 392: 202–212.

Bruns, T. D. 1995. "Thoughts on the Processes That Maintain Local Species Diversity of Ectomycorrhizal Fungi." *Plant and Soil* 170: 63–73.

Bunn, A. G. 2008. "A Dendrochronology Program Library in R (dplR)." *Dendrochronologia* 26, no. 2: 115–124. https://doi.org/10.1016/j.dendro.2008.01.002.

Bunn, A. G. 2010. "Statistical and Visual Crossdating in R Using the dplR Library." *Dendrochronologia* 28, no. 4: 251–258. https://doi.org/10.1016/j.dendro.2009.12.001.

Burke, D. J., A. J. Hoke, and J. Koch. 2020. "The Emergence of Beech Leaf Disease in Ohio: Probing the Plant Microbiome in Search of the Cause." *Forest Pathology* 50: 1–12.

Cale, J. A., M. T. Garrison-Johnston, S. A. Teale, and J. D. Castello. 2017. "Beech Bark Disease in North America: Over a Century of Research Revisited." *Forest Ecology and Management* 394: 86–103. https://doi.org/10.1016/j.foreco.2017.03.031.

Calic, I., J. Koch, D. Carey, C. Addo-Quaye, J. E. Carlson, and D. B. Neale. 2017. "Genome-Wide Association Study Identifies a Major Gene for Beech Bark Disease Resistance in American Beech (*Fagus Grandifolia* Ehrh.)." *BMC Genomics* 18, no. 1: 547. https://doi.org/10.1186/s12864-017-3931-z.

Canham, C. D. 1990. "Suppression and Release During Canopy Recruitment in *Fagus Grandifolia*." *Bulletin of the Torrey Botanical Club* 117: 1–7.

Carta, L. K., Z. A. Handoo, S. Li, et al. 2020. "Beech Leaf Disease Symptoms Caused by Newly Recognized Nematode Subspecies *Litylenchus Crenatae Mccannii* (Anguinata) Described From *Fagus Grandifolia* in North America." *Forest Pathology* 50: 1–15. https://doi.org/10.1111/efp.12580.

Castaño, C., E. Suarez-Vidal, R. Zas, J. A. Bonet, J. Oliva, and L. Sampedro. 2023. "Ectomycorrhizal Fungi With Hydrophobic Mycelia and Rhizomorphs Dominate in Young Pine Trees Surviving Experimental Drought Stress." *Soil Biology & Biochemistry* 178: 108932.

Chuste, P.-A., P. Maillard, N. Bréda, et al. 2020. "Sacrificing Growth and Maintaining a Dynamic Carbohydrate Storage Are Key Processes for Promoting Beech Survival Under Prolonged Drought Conditions." *Trees* 34: 381–394.

Druebert, C., C. Lang, K. Valtanen, and A. Polle. 2009. "Beech Carbon Productivity as Driver of Ectomycorrhizal Abundance and Diversity." *Plant, Cell & Environment* 32, no. 8: 992–1003.

Ewing, C. J., C. E. Hausman, J. Pogacnik, J. Slot, and P. Bonello. 2019. "Beech Leaf Disease: An Emerging Forest Epidemic." *Forest Pathology* 49: 1–4.

Ewing, C. J., J. Slot, M. S. Benitez, et al. 2021. "The Foliar Microbiome Suggests That Fungal and Bacterial Agents May Be Involved in the Beech Leaf Disease Pathosystem." *Phytobiomes Journal* 5: 335–349.

Fletcher, L. R., A. M. Borsuk, A. C. Fanton, et al. 2023. "Anatomical and Physiological Consequences of Beech Leaf Disease in *Fagus Grandifolia* L." *Forest Pathology* 54, no. 1: e12842. https://doi.org/10.1111/efp.12842.

Gardes, M., and T. D. Bruns. 1993. "ITS Primers With Enhanced Specificity for Basidiomycetes-Application to the Identification of Mycorrhizae and Rusts." *Molecular Ecology* 2, no. 2: 113–118.

Garnas, J. R., M. P. Ayres, A. M. Liebhold, and C. Evans. 2011. "Subcontinental Impacts of an Invasive Tree Disease on Forest Structure and Dynamics." *Journal of Ecology* 99, no. 2: 532–541. https://doi.org/10.1111/j.1365-2745.2010.01791.x.

Goraya, M., C. Kantor, P. Vieira, D. Martin, and M. Kantor. 2024. "Deciphering the Vectors: Unveiling the Local Dispersal of Litylenchus Crenatae ssp. Mccannii in the American Beech (*Fagus grandifolia*) Forest Ecosystem." *PLoS One* 19, no. 11: e0311830.

Hart, A. T., S. M. Landhausser, and E. Wiley. 2024. "Tracing Carbon and Nitrogen Reserve Remobilization During Spring Leaf Flush and Growth Following Defoliation." *Tree Physiology* 44: 145–157. https://doi.org/10.1093/treephys/tpae015.

Heberling, J. M., and R. M. Muzika. 2023. "Not All Temperate Deciduous Trees Are Leafless in Winter: The Curious Case of Marcescence." *Ecosphere* 14, no. 3: e4410.

Hill, A. L., J. G. Whitehill, S. O. Opiyo, P. L. Phelan, and P. Bonello. 2012. "Nutritional Attributes of Ash (Fraxinus spp.) Outer Bark and Phloem and Their Relationships to Resistance Against the Emerald Ash Borer." *Tree Physiology* 32, no. 12: 1522–1532.

Houston, D. R. 1975. "Beech Bark Disease–the Aftermath Forests Are Structured for a New Outbreak." *Journal of Forestry* 73, no. 10: 660–663.

Jakubas, W. J., C. R. McLaughlin, P. G. Jensen, and S. A. McNulty. 2005. "Alternate Year Beechnut Production and Its Influence on Bear and Marten Populations." In *Beech Bark Disease: Proceedings of the Beech Bark Disease Symposium; 2004 June 16-18; Saranak Lake, NY. Gen. Tech. Rep*, edited by C. A. Evans, J. A. Lucas, and M. J. Twery, 79–87. US. Department of Agriculture, Forest Service, Northeastern Research Station.

Kanzaki, N., Y. Ichihara, T. Aikawa, T. Ekino, and H. Masuya. 2019. "Litylenchus Crenatae n. sp. (Tylenchomorpha: Anguinidae), a Leaf Gall Nematode Parasitising Fagus Crenata Blume." *Nematology* 21: 5–22.

Karlsen-Ayala, E., M. A. Jusino, R. Gazis, and M. E. Smith. 2023. "Habitat Matters: The Role of Spore Bank Fungi in Early Seedling Establishment of Florida Slash Pines." *Fungal Ecology* 62: 101210. https://doi.org/10.1016/j.funeco.2022.101210.

Kasson, M. T., and W. H. Livingston. 2012. "Relationships Among Beech Bark Disease, Climate, Radial Growth Response and Mortality of American Beech in Northern Maine, USA." *Forest Pathology* 42: 199–212.

Leak, W. B. 2006. "Fifty-Year Impacts of the Beech Bark Disease in the Bartlett Experimental Forest, New Hampshire." *Nourthern Journal of Applied Forestry* 23, no. 2: 141–143.

Maxwell, R. S., and L.-A. Larsson. 2021. "Measuring Tree-Ring Widths Using the CooRecorder Software Application." *Dendrochronologia* 67: 125841. https://doi.org/10.1016/j.dendro.2021.125841.

Mcdowell, N. G., and S. Sevanto. 2010. "The Mechanisms of Carbon Starvation: How, When, or Does It Even Occur at All?" *New Phytologist* 186: 263–264.

McIntire, C. D. 2023. "Physiological Impacts of Beech Leaf Disease Across a Gradient of Symptom Severity Among Understory American Beech." *Frontiers in Forests and Global Change* 6: 1146742. https://doi.org/10.3389/ffgc.2023.1146742.

McIntire, C. D., and P. Vieira. 2025. "Phenological Evaluation of Bud Retention, Leaf Production, and Nematode Abundance Associated With Beech Leaf Disease." *Forest Pathology* 55, no. 2: e70014.

McNulty, S. A., and R. D. Masters. 2005. "Beech Bark Disease: Proceedings of the Beech Bark Disease Symposium; 2004 June 16-18; Saranak Lake, NY." In *Changes to the Adirondack Forest: Implications of Beech Bark Disease on Forest Structure and Seed Production*, edited by C. A. Evans, J. A. Lucas, and M. J. Twery, 52–57. US. Department of Agriculture, Forest Service, Northeastern Research Station.

Medvigy, D., K. L. Clark, N. S. Skowronski, and K. V. R. Schafer. 2012. "Simulated Impacts of Insect Defoliation on Forest Carbon Dynamics." *Environmental Research Letters* 7: 1–9.

Michaud, T. J., I. S. Pearse, H. Kauserud, C. J. Andrew, and P. G. Kennedy. 2024. "Mast Seeding in European Beech (*Fagus Sylvatica* L.) is Associated With Reduced Fungal Sporocarp Production and Community Diversity." *Ecology Letters* 27, no. 6: e14460.

Miles, P. D., and W. B. Smith. 2009. *Specific Gravity and Other Properties of Wood and Bark for 156 Tree Species Found in North America*. U.S. Department of Agriculture, Forest Service, Northern Research Station.

Oswald, S. W., and D. P. Aubrey. 2024. "Season of Drought Affects Growth, but Not Nonstructural Carbohydrates Dynamics, in *Pinus Taeda* Saplings." *Tree Physiology* 44: tpae014.

Papaik, M. J., C. D. Canham, E. F. Latty, and K. D. Woods. 2005. "Effects of an Introduced Pathogen on Resistance to Natural Disturbance: Beech Bark Disease and Windthrow." *Canadian Journal of Forest Research* 35, no. 8: 1832–1843. https://doi.org/10.1139/x05-116.

Peay, K. G., P. G. Kennedy, and T. D. Bruns. 2011. "Rethinking Ectomycorrhizal Succession: Are Root Density and Hyphal Exploration Types Drivers of Spatial and Temporal Zonation?" *Fungal Ecology* 4, no. 3: 233–240.

Pec, G. J., S. W. Simard, J. F. Cahill Jr., and J. Karst. 2020. "The Effects of Ectomycorrhizal Fungal Networks on Seedling Establishment Are Contingent on Species and Severity of Overstorey Mortality." *Mycorrhiza* 30, no. 2: 173–183.

Piper, F. I., M. J. Gundale, and A. Fajardo. 2015. "Extreme Defoliation Reduces Tree Growth but Not C and N Storage in a Winter-Deciduous Species." *Annals of Botany* 115: 1093–1103.

Plotkin, A. B., M. Blumstein, D. Laflower, et al. 2021. "Defoliated Trees Die Below a Critical Threshold of Stored Carbon." *Functional Ecology* 35, no. 10: 2156–2167. https://doi.org/10.1111/1365-2435.13891.

Pringle, E. G. 2016. "Integrating Plant Carbon Dynamics With Mutualism Ecology." *New Phytologist* 210, no. 1: 71–75.

PRISM Climate Group. 2024. "PRISM Climate Group, Oregon State University." https://prism.oregonstate.edu.

Puri, E., G. Hoch, and C. Körner. 2015. "Defoliation Reduces Growth but Not Carbon Reserves in Mediterranean *Pinus pinaster* Trees." *Trees* 29: 1187–1196.

R Core Team. 2025. "R: A Language and Environment for Statistical Computing." R Foundation for Statistical Computing. https://www.R-project.org/.

Reed, S. E., S. Greifenhagen, Q. Yu, et al. 2020. "Foliar Nematode, Litylenchus Crenatae Ssp. Mccannii, Population Dynamics in Leaves and Buds of Beech Leaf Disease-Affected Trees in Canada and the US." *Forest Pathology* 50: 1–9.

Reed, S. E., D. Volk, D. K. H. Martin, et al. 2022. "The Distribution of Beech Leaf Disease and the Causal Agents of Beech Bark Disease (*Cryptoccocus Fagisuga*, *Neonectria Faginata*, *N. Ditissima*) in Forests Surrounding Lake Erie and Future Implications." *Forest Ecology and Management* 503: 119753. https://doi.org/10.1016/j.foreco.2021.119753.

Richardson, A. D., M. S. Carbone, T. F. Keenan, et al. 2012. "Seasonal Dynamics and Age of Stemwood Nonstructural Carbohydrates in Temperate Forest Trees." *New Phytologist* 197: 850–861.

Rigsby, C. M., C. Villari, D. L. Peterson, D. A. Herms, P. Bonello, and D. Cipollini. 2019. "Girdling Increases Survival and Growth of Emerald Ash Borer Larvae on Manchurian Ash." *Agricultural and Forest Entomology* 21, no. 1: 130–135.

Sapes, G., P. Demaree, Y. Lekberg, and A. Sala. 2021. "Plant Carbohydrate Depletion Impairs Water Relations and Spreads via Ectomycorrhizal Networks." *New Phytologist* 229, no. 6: 3172–3183.

Saravesi, K., A. Markkola, P. Rautio, M. Roitto, and J. Tuomi. 2008. "Defoliation Causes Parallel Temporal Responses in a Host Tree and Its Fungal Symbionts." *Oecologia* 156: 117–123.

Schaefer, K. V., K. L. Clark, N. Skowronski, and E. P. Hamerlynck. 2010. "Impact of Insect Defoliation on Forest Carbon Balance as Assessed With a Canopy Assimilation Model." *Global Change Biology* 16: 546–560. https://doi.org/10.1111/j.1365-2486.2009.02037.x.

Schomaker, M. E., S. J. Zarnoch, W. A. Bechtold, D. J. Latelle, W. G. Burkman, and S. M. Cox. 2007. "USDA General Technical Reports SRS-102." In *Crown-Condition Classification: A Guide to Data Collection and Analysis*, 92. U.S. Department of Agriculture Forest Service.

Shepherd, B. L., D. J. Burke, and K. L. Stuble. 2025. "*Fagus grandifolia* Growth and Mortality a Decade After the Emergence of Beech Leaf Disease." *Trees, Forests and People* 20: 100836.

Smith, M. E., G. W. Douhan, and D. M. Rizzo. 2007. "Ectomycorrhizal Community Structure in a Xeric Quercus Woodland Based on rDNA Sequence Analysis of Sporocarps and Pooled Roots." *New Phytologist* 174, no. 4: 847–863.

Smith, S. E., and D. J. Read. 2010. *Mycorrhizal Symbiosis*. Academic Press.

Storer, A. J., J. N. Rosemier, B. L. Beachy, and D. J. Flaspohler. 2005. "Beech Bark Disease: Proceedings of the Beech Bark Disease Symposium; Saranak Lake, NY. General Technical Reports. NE-331." In *Potential Effects of Beech Bark Disease and Decline in Beech Abundance on Birds and Small Mammals*, edited by C. A. Evans, J. A. Lucas, and M. J. Twery, 72–78. Department of Agriculture, Forest Service, Northeastern Research Station.

Tang, Y., M. Horikoshi, and W. Li. 2016. "Ggfortify: Unified Interface to Visualize Statistical Result of Popular R Packages." *R Journal* 8, no. 2: 474–485. https://doi.org/10.32614/RJ-2016-060.

Taylor, A. R., D. A. McPhee, and J. A. Loo. 2013. "Incidence of Beech Bark Disease Resistance in the Eastern Acadian Forest of North America." *Forestry Chronicle* 89: 690–695.

Taylor, D., and T. Bruns. 1999. "Community Structure of Ectomycorrhizal Fungi in a *Pinus muricata* Forest: Minimal Overlap Between the Mature Forest and Resistant Propagule Communities." *Molecular Ecology* 8, no. 11: 1837–1850.

Vandepol, N., J. Liber, A. Desiro, et al. 2020. "Resolving the Mortierellaceae Phylogeny Through Synthesis of Multi-Gene Phylogenetics and Phylogenomics." *Fungal Diversity* 104, no. 1: 267–289. https://doi.org/10.1007/s13225-020-00455-5.

Vieira, P., M. R. Kantor, A. Jansen, Z. A. Handoo, and J. D. Eisenback. 2023. "Cellular Insights of Beech Leaf Disease Reveal Abnormal Ectopic Cell Division of Symptomatic Interveinal Leaf Areas." *PLoS One* 18, no. 10: e0292588. https://doi.org/10.1371/journal.pone.0292588.

Vilgalys, R., and M. Hester. 1990. "Rapid Genetic Identification and Mapping of Enzymatically Amplified Ribosomal DNA From Several Cryptococcus Species." *Journal of Bacteriology* 172, no. 8: 4238–4246.

Wang, Z., Z. Zhou, and C. Wang. 2021. "Defoliation-induced tree growth declines are jointly limited by carbon source and sink activities" *Science of the Total Environment* 762: 143077.

Wiley, E., S. Huepenbecker, B. B. Casper, and B. R. Helliker. 2013. "The Effects of Defoliation on Carbon Allocation: Can Carbon Limitation Reduce Growth in Favour of Storage ?" *Tree Physiology* 33: 1216–1228.

Supporting Information

Additional supporting information can be found online in the Supporting Information section. **Data S1:** efp70068-sup-0001-Supinfo01.docx.